Tenth International Conference on Computational Fluid Dynamics (ICCFD10), Barcelona, Spain, July 9-13, 2018

ICCFD10-032

Numerical Calculations of the Dynamic Behavior of Hydrogen-Air Lean Premixed Flames due to Intrinsic Instability Based on the Detailed Chemical Reaction Model

S. Kadowaki*, R. Ohki*, Thwe Thwe Aung**, T. Katsumi* and H. Kobayashi***
Corresponding author: kadowaki@mech.nagaokaut.ac.jp

* Nagaoka University of Technology, Japan
** Japan Atomic Energy Agency, Japan
*** Tohoku University, Japan

Abstract: The dynamic behavior of hydrogen-air lean premixed flames due to intrinsic instability was numerically investigated by two-dimensional unsteady calculations of reactive flows. We used the compressible Navier-Stokes equations with the detailed hydrogen-oxygen combustion consisting of seventeen elementary reversible reactions of eight reactive species and a nitrogen diluent. We obtained the critical wavelength through the dispersion relation, which was closely related with the dynamic behavior of premixed flames due to intrinsic instability. To investigate the characteristics of dynamic behavior, the disturbance with the critical wavelength was superimposed on premixed flames. The superimposed disturbance evolved owing to intrinsic instability, and then the cellular-flame front formed. With an increase in the space size, the burning velocity of a cellular flame became monotonously larger, which was generated by disturbances with long wavelengths. This indicated that the scale effect affected strongly the increase in the burning velocity. In addition, we found that the concentrations of hydrogen and hydroxyl radicals were high (low) in the downstream region of convex (concave) flame fronts with respect to the unburned gas. This was due to the diffusive-thermal effect. Moreover, we obtained the fractal dimension of flame fronts to elucidate the dynamic behavior of premixed flames. We revealed the scale effect on the burning velocity and the role of intermediate species in cellular flames to clarify the essence of intrinsic instability.

Keywords: Lean premixed combustion, Hydrogen flame, Intrinsic instability, Scale effect, Intermediate species

1 Introduction

Now we focus on the significance of lean combustion of hydrogen-air premixtures to reduce emissions of carbon dioxide and nitrogen oxide. It is well known that hydrogen-air lean premixed flames become unstable owing to intrinsic instability, i.e. hydrodynamic instability and diffusive-thermal instability [1]. In practical applications of hydrogen-based lean combustion systems, we have to control the dynamic behavior of hydrogen-air lean premixed flames due to intrinsic instability. Thus, the clarification of intrinsic instability is critically significant to the practical implementation of lean combustion systems based on hydrogen.

Hydrodynamic instability caused by thermal expansion is essential to the intrinsic instability of all premixed flames, and diffusive-thermal instability caused by preferential diffusion of mass versus heat

affects the intrinsic instability of hydrogen-air lean premixed flames [2-6]. Intrinsic instability has a great influence on the dynamic behavior of premixed flames. Thus, we shall obtain the fundamental knowledge of intrinsic instability to control effectively hydrogen-air lean premixed flames.

Numerical approach is effective to clarify the essence of intrinsic instability of premixed flames. In previous numerical researches, the fundamental mechanism of intrinsic instability was elucidated [7-12]. In addition, the scale effect on the dynamic behavior of premixed flames was estimated through the numerical results based on the one-step chemical reaction model [13-14] where the role of intermediate species was disregarded. However, intermediate species play an important role in the characteristics of hydrogen-air flames [15-16]. Thus, it is necessary to adopt detailed chemical reaction model in numerical calculations to understand the role of intermediate species in the dynamic behavior of hydrogen-air flames.

We performed numerical calculations of hydrogen-air lean premixed flames based on the detailed chemical reaction model. The burning velocity of a cellular flame depending on the space size was obtained to estimate the scale effect. The role of intermediate species in cellular flames was examined. In addition, the fractal dimension of flame fronts was obtained to elucidate the dynamic behavior of premixed flames.

2 Governing Equations

We adopted the reaction mechanism for hydrogen oxidation proposed by Westbrook [17] which is modeled with seventeen elementary reversible reactions of eight reactive species, H_2, O_2, H, O, OH, HO_2, H_2O_2, H_2O, and N_2 as a diluent.

To get the transport coefficients of pure gases, we used the formulae founded on the rigorous kinetic theory [18]. Thermal conductivity, dynamic viscosity, and diffusion coefficients of each species in gaseous mixtures were obtained by the mixture rules [19-21].

The body force, radiation, bulk viscosity, Soret effect, Dufour effect, and pressure gradient diffusion were neglected in numerical calculations. We considered two-dimensional unsteady reactive flows and took the direction tangential to the flame front as the *y*-direction, with the gas velocity in the positive *x*-direction.

The goverining equations are written in the conservation form as:

$$\frac{\partial}{\partial t}(\rho Y_i)+\frac{\partial}{\partial x}\left(\rho Y_i u-\rho D_i\frac{\partial Y_i}{\partial x}\right)+\frac{\partial}{\partial y}\left(\rho Y_i v-\rho D_i\frac{\partial Y_i}{\partial y}\right)=w_i \tag{1}$$

$$\frac{\partial}{\partial t}(\rho)+\frac{\partial}{\partial x}(\rho u)+\frac{\partial}{\partial y}(\rho v)=0 \tag{2}$$

$$\frac{\partial}{\partial t}(\rho u)+\frac{\partial}{\partial x}\left\{\rho u^2+p-\mu\left(\frac{4}{3}\frac{\partial u}{\partial x}-\frac{2}{3}\frac{\partial v}{\partial y}\right)\right\}+\frac{\partial}{\partial y}\left\{\rho uv-\mu\left(\frac{\partial v}{\partial x}+\frac{\partial u}{\partial y}\right)\right\}=0 \tag{3}$$

$$\frac{\partial}{\partial t}(\rho v)+\frac{\partial}{\partial x}\left\{\rho uv-\mu\left(\frac{\partial v}{\partial x}+\frac{\partial u}{\partial y}\right)\right\}+\frac{\partial}{\partial y}\left\{\rho v^2+p-\mu\left(\frac{4}{3}\frac{\partial v}{\partial y}-\frac{2}{3}\frac{\partial u}{\partial x}\right)\right\}=0 \tag{4}$$

$$\begin{aligned}&\frac{\partial}{\partial t}(\rho e_t)+\frac{\partial}{\partial x}\left\{(\rho e_t+p)u-\kappa\frac{\partial T}{\partial x}-\sum_i\left(h_i\rho D_i\frac{\partial Y_i}{\partial x}\right)\right\}\\&\quad+\frac{\partial}{\partial y}\left\{(\rho e_t+p)v-\kappa\frac{\partial T}{\partial y}-\sum_i\left(h_i\rho D_i\frac{\partial Y_i}{\partial y}\right)\right\}=0\end{aligned} \tag{5}$$

$$p = \left(\sum_i C_i \right) RT \tag{6}$$

where ρ is the density, Y is the mass fraction, u and v are x and y components of velocity, p is the pressure, e_t is the stored energy, T is the temperature, C is the molecular concentration, D is the effective diffusion coefficient, w is the mass rate of production, μ is the dynamic viscosity, κ is the thermal conductivity, h is the enthalpy, R is the universal gas constant, and the subscript i denotes the i-th species.

3 Numerical Procedures

Hydrogen-air lean premixed flames with the equivalence ratio of 0.5 were treated, and the temperature and pressure of the unburned gas were assumed to be 298 K and 1.013×10^5 Pa, respectively. The calculated burning velocity under the adiabatic conditions was 0.503 m/s.

Initial conditions for disturbed flames were provided with the solutions of stationary planar flames. On a planar flame, we superimposed a sinusoidal disturbance with the initial amplitude A_0 and the wavelength λ. The displacement of the flame front in the x-direction due to the disturbance was given by

$$A_0 \sin(2\pi y/\lambda) \tag{7}$$

Boundary conditions were as follows: In the x-direction, the free-flow conditions were used upstream and downstream, and the one-sided difference approximation with second-order accuracy was appropriated. The inlet-flow velocity was set equal to the burning velocity of a planar flame. In the y-direction, the spatially periodic conditions were used.

The explicit MacCormack scheme, which has second-order accuracy in both time and space, was adopted for numerical calculations. A computational domain was 50 mm in the x-direction (L_x) and N times wavelength in the y-direction (L_y), which was resolved by $1851 \times (32N + 1)$ spaced grid. We set N = 1, 2, 4, 8 and 12, and confirmed that the numerical results were independent of L_x. The minimum grid size in the x-direction was set to 0.02 mm, and the used grid was fine enough to prevent numerical errors from contaminating the solutions. The time-step interval was 10 ns.

4 Results and Discussion

Figure 1 shows the dynamic behavior of premixed flames at $L_y = 4\lambda_c$, $8\lambda_c$ and $12\lambda_c$, where λ_c is the critical wavelength corresponding to the linearly most unstable wavelength. The unburned gas flows in from the left, and the burned gas flows out to the right. Disturbances superimposed on flames evolve, and then cellular-flame fronts appear. This is due to intrinsic instability, i.e. hydrodynamic instability and diffusive-thermal instability. The shapes of flame fronts change drastically with time, and we observe 2, 4 and 6 cells at $L_y = 4\lambda_c$, $8\lambda_c$ and $12\lambda_c$, respectively.

A cellular flame has wider surface area, so that the burning velocity of a cellular flame (S_{cf}) is larger than that of a planar flame (S_u). Figure 2 shows the normalized burning velocities of cellular flames, depending on L_y / λ_c. The normalized burning velocity increases monotonously as the space size becomes larger, which is generated by disturbances with long wavelengths. We understand that the long-wavelength components of disturbances have a great influence on the increase in the burning velocity. The obtained results indicate that the scale effect affects strongly dynamic behavior of premixed flames.

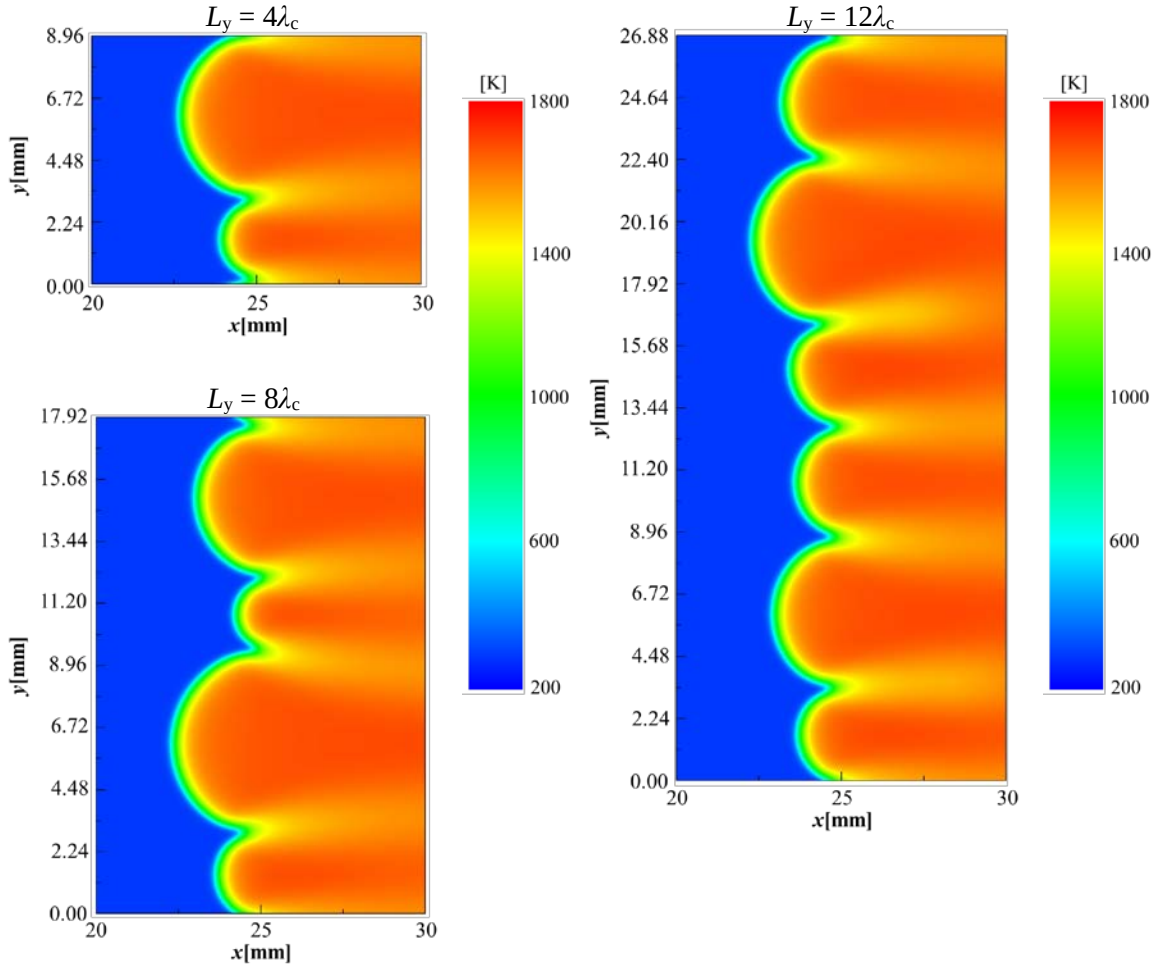

Fig. 1: Dynamic behavior of premixed flames at $L_y = 4\lambda_c$, $8\lambda_c$ and $12\lambda_c$.

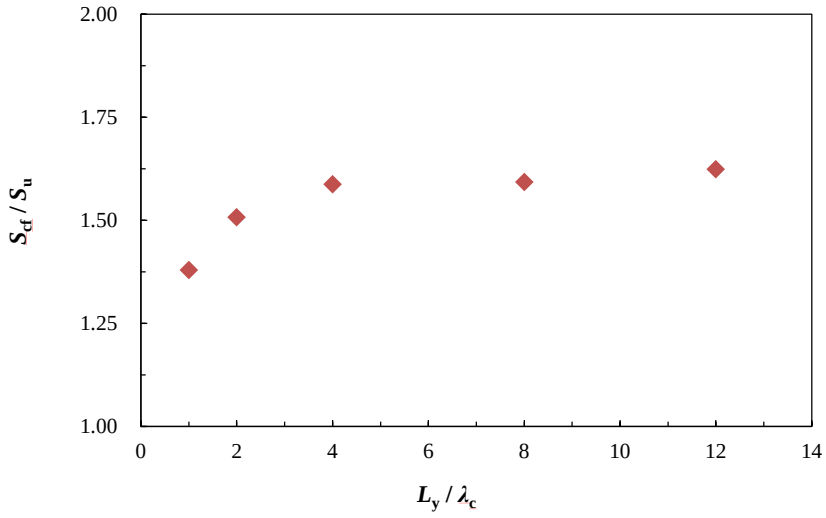

Fig. 2: Normalized burning velocities of cellular flames.

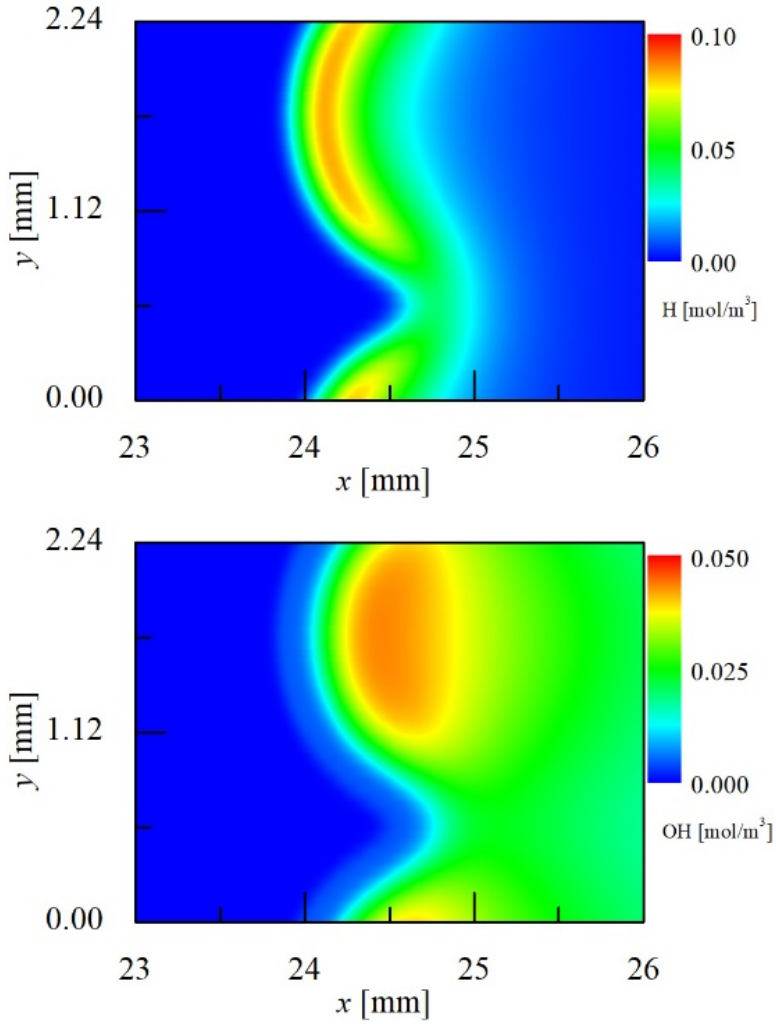

Fig. 3: Distributions of hydrogen radical (upper) and hydroxyl radical (lower).

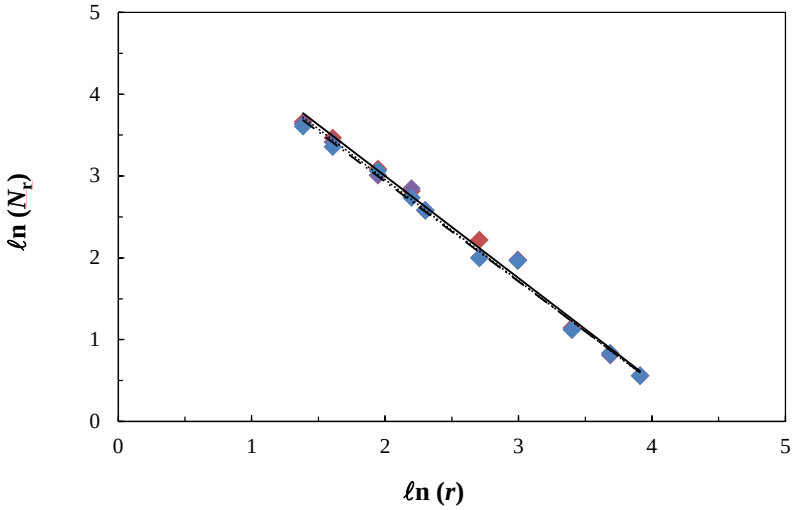

Fig. 4: Relations between the number of circles N_r and the radius of circles r by the box counting method in fractal analysis.

Figure 3 shows the distributions of hydrogen radical (upper) and hydroxyl radical (lower). We find high concentrations of hydrogen and hydroxyl radicals in the downstream region of convex flame fronts with respect to the unburned gas. This is because that the downstream region has high temperature due to the diffusive-thermal effect. In the downstream region of 'concave' flame fronts, on the other hand, the temperature is low. Therefore, the concentrations of hydrogen and hydroxyl radicals are high (low) in the downstream region of convex (concave) flame fronts.

To obtain the fractal dimension of flame fronts, we perform the fractal analysis adopting the box counting method. Figure 4 shows the relations between the number of circles N_r and the radius of circles r for cellular flame fronts at $L_y = 12\lambda_c$ (t = 4.3, 4.5 and 4.7 ms). From the gradients of lines, we obtain the fractal dimension, $D \simeq 1.24$, which is independent of the time.

5 Conclusions

We have investigated numerically the dynamic behavior of hydrogen-air lean premixed flames due to intrinsic instability, based on the compressible Navier-Stokes equations with the detailed hydrogen-oxygen combustion consisting of seventeen elementary reversible reactions of eight reactive species and a nitrogen diluent. The obtained results are as follows:

1. The superimposed disturbance on a premixed flame evolves owing to intrinsic instability, and then the cellular-flame front forms. The shapes of flame fronts change drastically with time.
2. The burning velocity of a cellular flame increases monotonously as the space size becomes larger. This indicates that the scale effect affects strongly the increase in the burning velocity.
3. We find that the concentrations of hydrogen and hydroxyl radicals are high (low) in the downstream region of convex (concave) flame fronts with respect to the unburned gas. This is due to the diffusive-thermal effect.
4. We obtain the fractal dimension of flame fronts to elucidate the dynamic behavior of premixed flames, $D \simeq 1.24$. This value is independent of the time.

The scale effect on the dynamic behavior and the role of intermediate species in cellular flames are revealed to clarify the essence of intrinsic instability. The heat loss appears in practical applications and affects the dynamic behavior of hydrogen flames. In the near future, therefore, we will perform numerical calculations of hydrogen-air premixed flames taking account of the heat loss which has a great influence on intrinsic instability, especially diffusive-thermal instability.

References

[1] Williams, F. A., Combustion Theory, 2nd Edition, Addison-Wesley, 1985.

[2] Sivashinsky, G. I., Instabilities, pattern formation, and turbulence in flames, Ann. Rev. Fluid Mech., 15, 1983, 179-199.

[3] Clavin, P., Dynamic behavior of premixed flame fronts in laminar and turbulent flows, Prog. Energy Combust. Sci., 11, 1985, 1-59.

[4] Hertzberg, M., Selective diffusional demixing: occurrence and size of cellular flames, Prog. Energy Combust. Sci., 15, 1989, 203-239.

[5] Mitani, T. and Williams, F. A., Studies of cellular flames in hydrogen-oxygen-nitrogen mixtures, Combust. Flame, 39, 1980, 169-190.

[6] Qin, X., Kobayashi, H. and Niioka, T., Laminar burning velocity of hydrogen-air premixed flames at elevated pressure, Expr. Thermal Fluid Sci., 21, 2000, 58-63.

[7] Denet, B. and Haldenwang, P., Numerical study of thermaldiffusive instability of premixed flames, Combust. Sci. Technol., 86, 1992, 199-221.

[8] Bayliss, A. and Matkowsky, B. J., From traveling waves to chaos in combustion, SIAM J. Appl. Math., 54, 1994, 147-174.
[9] Daumont, I., Kassner, K., Misbah, C., and Valance, A., Cellular selfpropulsion of two-dimensional dissipative structures and spatial-period tripling Hopf bifurcation, Phys. Rev. E, 55, 1997, 6902-6906.
[10] Denet, B. and Haldenwang, P. A., Numerical study of premixed flames Darrieus–Landau instability, Combust. Sci. Technol., 104, 1995, 143-167.
[11] Senchenko, S., Bychkov, V., and Liberman, M., Stability limits of curved stationary flames in cylindrical tubes, Combust. Sci. Technol., 166, 2001, 109-130.
[12] Kadowaki, S. and Hasegawa, T., Numerical simulation of dynamics of premixed flames: flame instability and vortex-flame interaction, Prog. Energy Combust. Sci., 31, 2005, 193-241.
[13] Kadowaki, S., Takahashi, H., and Kobayashi, H., The effects of radiation on the dynamic behavior of cellular premixed flames generated by intrinsic instability, Proc. Combust. Inst., 33, 2011, 1153-1162.
[14] Kadowaki, S., Yanagioka, T., Yamazaki, W., and Kobayashi, H., The intrinsic instability of three-dimensional premixed flames under the low- and high-temperature conditions: effects of unburned-gas temperature on hydrodynamic and diffusive-thermal instabilities, Combust. Sci. Technol., 187, 2015, 1167-1181.
[15] G. Patnaik, G. and Kailasanath, K., Numerical simulations of burner-stabilized hydrogen-air flames in microgravity, Combust. Flame, 99, 1994, 247-253.
[16] Matsugi, A. and Terashima, H., Diffusive-thermal effect on local chemical structures in premixed hydrogen–air flames, Combust. Flame, 179, 2017, 238-241.
[17] Westbrook, C. K., Hydrogen oxidation kinetics in gases detonations, Combust. Sci. Technol., 29, 1982, 67-81.
[18] Hirschfelder, J. O., et al., Molecular Theory of Gases and Liquids, John Wiley & Sons, 1964.
[19] Wilke, C. R., A viscosity equation for gas mixtures, J. Chem. Phys., 18, 1950, 517-519.
[20] Coffee, T. P. and Heimerl, J. M., Transport algorithms for premixed, laminar steady-state flames, Combust. Flame, 43, 1981, 273-289.
[21] Wilke, C. R., Diffusional properties of multicomponent gases, Chem. Eng. Prog., 46, 1950, 95-104.